International Journal of Recent Technology and Engineering (IJRTE)
ISSN: 2277-3878 (Online), Volume-11 Issue-5, January 2023

Translational Calibration for Contact Type Three-Dimensional Position-Measuring Instruments

Hirofumi Maeda

Abstract*: In Japan, as the number of sewerage management facilities increases, continuous maintenance of drainage pipes and sewage pipes is considered important. However, it is grinding for operators to perform the expansive in-pipe inspection. Therefore, in recent years, inspections using stand-alone type piping inspection robots have been actively used. Inside of the pipe, there are disturbances such as unevenness, sludge, or dents at pipe joints which cause slips and tumbles of the robot. Therefore, the conventional ways of approaching those disturbances have been adjusting the size of the robot and tires according to the diameter of the pipe to prevent tipping over. We are exploring tip-over prevention measures by the software approach through advanced straight-ahead control. Currently, we are in the stage of verifying the self-position estimation necessary to realize straight-ahead control, and equipment for that purpose is required. However, to measure the position and posture of the robot inside the curved pipe, a special three-dimensional position-measuring device is required. Therefore, we have developed a three-dimensional position-measuring instrument for pipe inspection robots, but there is still an error in the absolute positioning accuracy. In this paper, to solve this error problem and make it precise, we propose a method to apply the calibration method used in the manipulator to the measuring instrument. Also, the kinematic model and its calibration parameters are explained, and a method of deleting unnecessary redundant parameters and parameter estimation by Newton's method is presented. Furthermore, in a comparative verification using a measuring instrument proposed in the paper, the positional accuracy after calibration is within a range of approximately ±1.0 mm, and the variation is also within a range of ±0.5 mm, which shows that the proposed method is effective.

***Keywords*: Measuring Instrument, Calibration, Contact Type, Exploration Robot, Water Pipe**

I. INTRODUCTION

Since 1965, sewerage development has been carried out in Japan. However, with the increase in the number of management facilities, the aging of long-term-use facilities is regarded as a problem. The standard service life of a sewer pipe is assumed to be 50 years. In addition, the possibility of road subsidence increases 30 years after the pipes are laid, which requires continuous maintenance.

Manuscript received on 01 December 2022 | Revised Manuscript received on 07 December 2022 | Manuscript Accepted on 15 January 2023 | Manuscript published on 30 January 2023.
* Correspondence Author (s)
Hirofumi Maeda*, Department of Information Science and Technology, National Institute of Technology (KOSEN), Yuge College, Ehime Prefecture, Japan. Email: maeda@info.yuge.ac.jp, ORCID ID: https://orcid.org/0000-0002-7145-3889

Therefore, inspections using robots have been actively performed for wide-range pipe inspection and to reduce the workload of field operators [1]. Typically, robot-using inspection is conducted with a wired remote-control method, in which a transport vehicle for operation is set near a manhole, and only the self-propelled vehicle, which is the main body of the robot, is put into the pipe. This method can reduce the weight of the main body by installing only the minimum functions necessary for driving in the self-propelled vehicle. In addition, since the operator controls and monitors the robot from the ground via a cable, this method has the advantage of being able to respond immediately to unforeseen contingencies. On the other hand, the place for setting the transport vehicle and field operators for wide-range intrusion control are required.

Therefore, in recent years, inexpensive lightweight stand-alone type pipe inspection robots have become the mainstream for the inspection. However, the stand-alone type is still under development, and research has not made much progress. In addition, in Japan, the minimum inspection diameter is 150 mm, whereas in other countries, the standard diameter is 200 mm or more, which makes it impossible to use those overseas products [2] [3] [4]. Under such circumstances, we have been conducting research and development aiming at the practical application of an autonomous pipe inspection robot that is compact and easy to carry [5] [6] [7] [8] [9].

To develop an autonomous pipe inspection robot, it is necessary to implement a function that prevents the robot body itself from tipping over inside the pipe. There are disturbances such as unevenness, sludge, or dents at pipe joints which cause slips and tumbles of the robot inside of a pipe. As for the conventional wired operating way, the operator controls the robot through the monitor as mentioned above so that unexpected contingency can be handled instantaneously. On the other hand, the stand-alone type must be equipped with a tipping-over prevention function in addition to the main inspecting function. The conventional ways of approaching those disturbances and preventing tipping over have been adjusting the size of the robot and tires according to the diameter of the pipe. We are exploring preventive measures by the software approach through advanced straight-ahead control. we are exploring the software approach by advanced straight-ahead control [10]-[11]. Currently, we are in the stage of verifying the self-position estimation necessary to realize straight-ahead control, and equipment for that purpose is required. However, to measure the position and posture of the robot inside the curved pipe, a special three-dimensional position-measuring device is required.

Therefore, we have developed a three-dimensional position-measuring instrument for pipe inspection robots [12] [13] [14] [15] [16] [17] [18]. This measuring instrument is a contact type to achieve high accuracy and precision. Since the contact type touches the object directly, it is highly accurate and reliable, but on the other hand, the structure of the equipment tends to be complicated, and the number of parts increases. For this reason, errors due to assembly, machining, encoder offset, etc. that occur between each rotating axis are accumulated, which leads to a large error in the absolute positioning accuracy. In this paper, to solve this error problem, we propose a method to apply the calibration method used in the manipulator to the contact type three-dimensional position measuring instrument. In addition, the structure of the measuring instrument is shown, and the measurement results before and after calibration and comparative verification are shown.

II. THE CONTACT TYPE THREE-DIMENSIONAL POSITION MEASURING INSTRUMENT

Verification of the pipe inspection robot is performed by suspending a contact-type three-dimensional position measuring instrument from directly above the half cut open pipe. The measurement structure and system configuration are shown below.

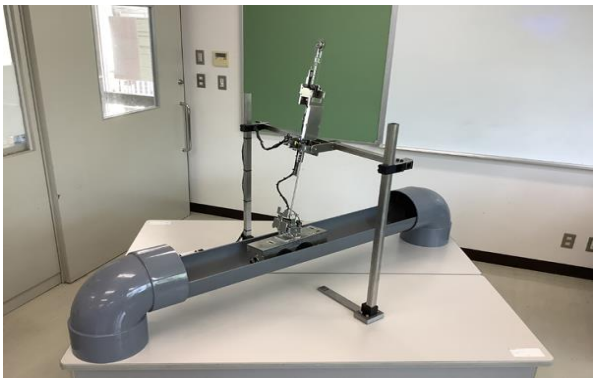

Fig. 1 Measuring the Position and Posture of the Piping Inspection Robot

A. Measurement Structure

This measuring instrument has 6 degrees of freedom as shown in Figure 2, and encoders are attached to each joint. Each joint is marked as J_1 to J_6 in order from the mounting frame as shown in Figure 3. J_3 is a translational joint and the others are rotational joints. In addition, a 6-axis stage is installed under the measuring instrument for accuracy verification (Figure 4).

Fig. 2 Appearance of Contact Type Three-Dimensional Position Measuring Instrument

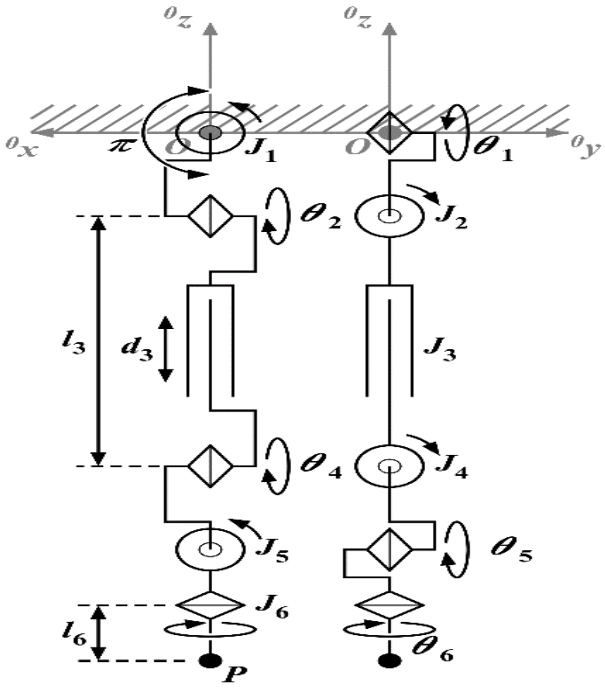

J_1-J_6 : the position of each joint
P : the position of the end effector
$\theta_1, \theta_2, \theta_4$-$\theta_6$: θ_1 to θ_6 excluding θ_3 each indicates the rotation angles for J_1 to J_6 excluding J_3 [rad]
d_3 : d_3 indicates the displacement for J_3 [m]
l_3 : l_3 indicates the initial link length for J_3 [m]
l_6 : link length of the end effector [m]
※ The joint pair of J_1 and J_2 shares the same axis, so do the another joint pair of J_4, J_5 and J_6, which leads to there is no link length between each joint pair.

Fig. 3 Link Structure of Contact Type Three-Dimensional Position Measuring Instrument

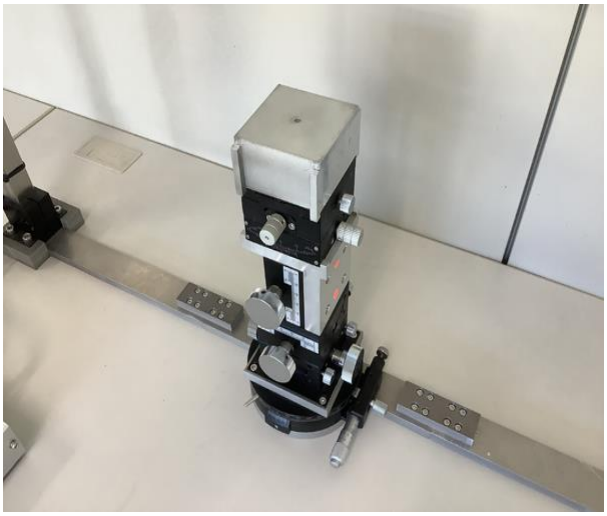

Fig. 4 6-Axis Stage for Accuracy Verification

Retrieval Number: 100.1/ijrte.E73840111523
DOI: 10.35940/ijrte.E7384.0111523
Journal Website: www.ijrte.org

Published By:
Blue Eyes Intelligence Engineering and Sciences Publication (BEIESP)

A pipe inspection robot is affected by two disturbances from the connecting part of the measuring instrument: “the self-weight of the measuring instrument on the robot” and “the moment of inertia around the joint between the measuring instrument and the robot.” In the verification of a pipe inspection robot, it is sufficient to reduce the disturbance to the extent that it does not affect the driving of the robot, that is, to the extent that it is sufficiently smaller than the torque generated by the robot itself.

Therefore, by attaching a pulley to the 2nd link, the disturbance against “the self-weight of the measuring instrument on the robot” can be reduced to 0 as much as possible (Figure 5). A weight with the same mass as the 3rd link to the tip of the measuring instrument is suspended on the pully with a wire. As a result, the entire weight of the measuring instrument always rests on its mounting frame, so there is no load on the pipe inspection robot.

Regarding “the moment of inertia around the joint between the measuring instrument and the robot,” by aligning the axis of rotation around each joint with the center of mass of the measuring instrument attached to that joint, the moment of inertia around the connection between the measuring instrument and the robot is minimized. As a result, only the moment of inertia of each joint when rotating around the axis passing through the center of gravity of the measuring instrument at each joint remains as a disturbance to the robot, but the load is small and can be ignored because the measuring instrument itself is lightweight.

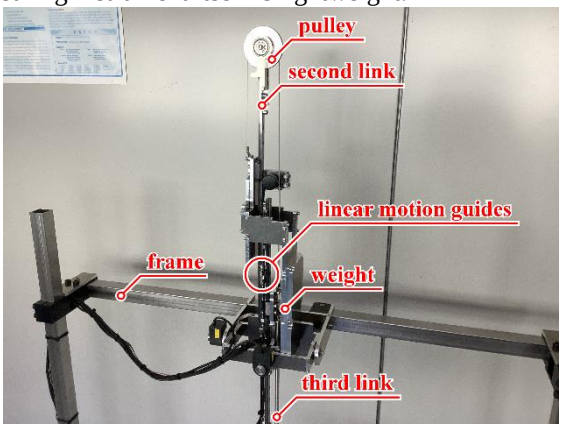

Fig. 5 Mounting Part and Pulley Part of Contact Type Three-Dimensional Position Measuring Instrument

B. System Configuration

This measuring instrument calculates the position and posture of the robot attached to the tip of the measuring instrument from the sensor values of the encoders attached to each joint (Figure 6). STK-7125 manufactured by Alpha Project Co., Ltd. is used to acquire the encoder (Figure 7). UN-2000 and DX-025 of Mutoh Industries, Ltd. are used as encoders. After connecting STK-7125 with an open collector, the angle of rotation is calculated from the difference between the A phase and B phase in the phase counting mode. After that, the encoder value obtained by STK-7125 is sent to the iPad via BLE. Finally, each joint angle is derived and accumulated from the encoder values on the iPad, and the robot's position and posture are calculated based on that data by forward kinematics (Figure 8). The details of the forward kinematics are omitted here as they are described in Reference 18.

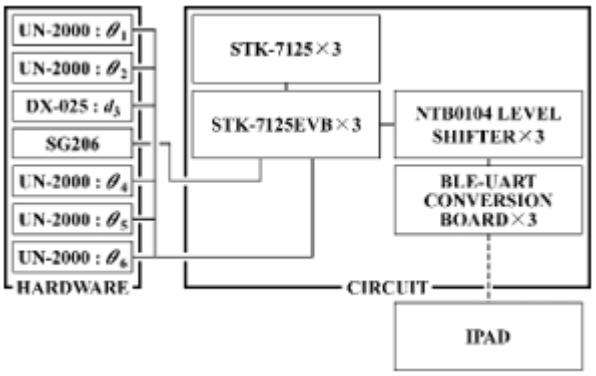

Fig. 6 Schematic Diagram of the System

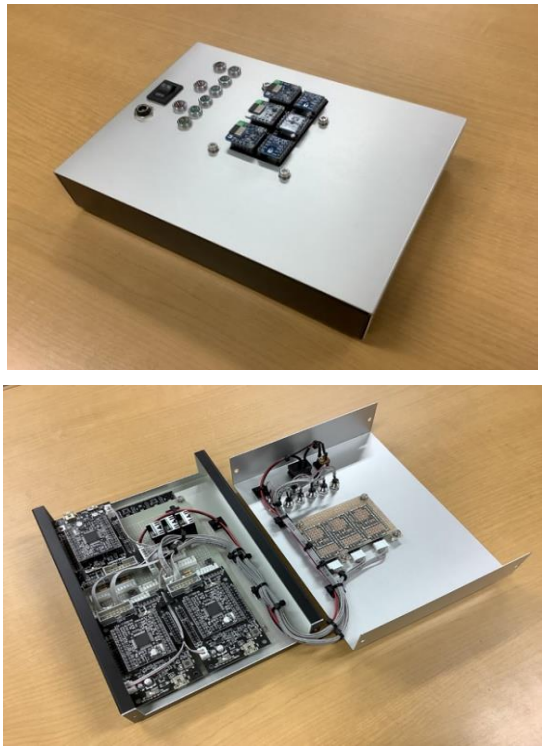

Fig. 7 The Control Circuit of the Measuring Instrument

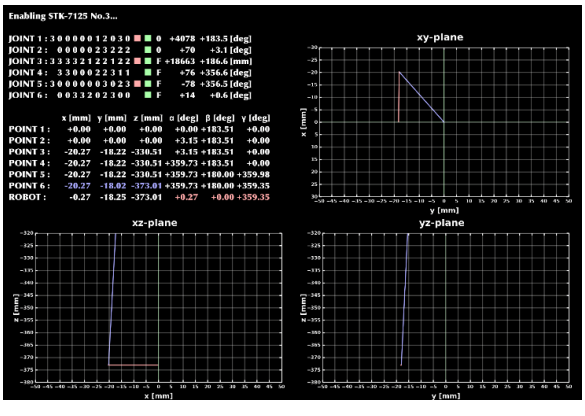

Fig. 8 Drawing Screen of Measurement Results on IPad

III. CALIBRATION METHOD

Here, we show how to apply the manipulator calibration method performed by Ishii et al. to the measuring instrument [19].

Published By:
Blue Eyes Intelligence Engineering and Sciences Publication (BEIESP)

A. Kinematic Model and Calibration Parameters

The calibration of the measuring instrument requires the configuration of the kinematic model and the setting of its parameters. Therefore, in this study, we set up a general coordinate system with 6 degrees of freedom for each rotating axis as a kinematic model of the measuring instrument. Since the translation and rotation on each axis between adjacent coordinate systems are the parameters to be calibrated, we can obtain a conversion formula with six parameters of position and posture between each adjacent coordinate system. In other words, since this instrument has 6 degrees of freedom, the kinematic model is composed of 36 parameters.

Now, consider θ_1, θ_2, d_3, θ_4 to θ_6 in Fig. 3 and the offset value of each encoder. The relationship between the encoder value E_i and the rotation angle θ_i at each joint is given by Equation (1), and the relationship between the encoder value E_3 and displacement d_3 at joint J_3 is given by Equation (2).

$$E_i = C_i \cdot \theta_i + O_i \quad (i = 1, 2, 4, 5, 6) \tag{1}$$

$$E_3 = C_3 \cdot d_3 + O_3 \tag{2}$$

Where C_i is the known constant of proportionality and O_i is the offset value of the encoder. Also, if E_i (i = 1 to 6) can be detected, O_i can be converted to the target parameter for calibration.

B. Setting Calibration Parameters

In the kinematic model based on the vector notation used in this study, there are functional overlaps in translation and rotation between each coordinate system, and redundancy occurs in the parameters. Therefore, it is necessary to delete those unnecessary redundant parameters.

First, place a point P_a on the tip of the measuring instrument as a measurement reference point for calibration. Next, if $\boldsymbol{q}$ is a vector whose elements are n unknown parameters, the relationship between vector $\boldsymbol{p}$ (3×1) representing the position of reference point P_a and vector $\boldsymbol{q}$ can be expressed by equation (3).

$$\boldsymbol{p} = f(\boldsymbol{q}) \tag{3}$$

In addition, when $\Delta\boldsymbol{p}$ is the deviation between the measured value of the reference point P_a based on the parameters of the kinematic model and the measured value, $\Delta\boldsymbol{p}$ is approximated by the sum of the linear combinations of the small fluctuations of each parameter, so it can be expressed by Equation (4).

$$\Delta\boldsymbol{p} = (\partial\boldsymbol{p}/\partial\boldsymbol{q}) \cdot \Delta\boldsymbol{q} = A \cdot \Delta\boldsymbol{q} \tag{4}$$

Where A represents the Jacobian matrix (3×n) with respect to the parameters. Furthermore, if we obtain the position data for m points P_a, we can obtain the vector $\boldsymbol{r}$ (3 m ×1) corresponding to these and its extended Jacobean matrix B(3m×n), so that equation (5) holds.

$$\Delta\boldsymbol{r} = B \cdot \Delta\boldsymbol{q} \tag{5}$$

Also, $\Delta\boldsymbol{r}$ and B are $\Delta\boldsymbol{r} = \left[\Delta\boldsymbol{p}_1^T \quad \Delta\boldsymbol{p}_2^T \quad \cdots \quad \Delta\boldsymbol{p}_m^T\right]^T$ and $B = [A_1^T \quad A_2^T \quad \cdots \quad A_m^T]^T$ respectively. In order for the inverse transformation of B to exist, more than 1/3 of n measurements are required.

Here, B is constructed by substituting the measured value of the reference point P_a at different positions and postures of the measuring instrument, the offset value of the encoder, and the initial values of each parameter into the obtained equation (5). Next, since the elements of B include length and angles, the gap between each value becomes large, so the elements are normalized using appropriate numerical values. In this study, we used the square root of the sum of squares of the elements in each column of B as an appropriate numerical value. Next, find the pseudo-inverse of the normalized matrix B. Equation (6) shows how to obtain a general pseudo-inverse matrix B^*.

$$B^* = \left[B^T B\right]^{-1} B^T \tag{6}$$

When Equation (6) is used, the value of $\left[B^T B\right]^{-1}$ may diverge depending on the state of B. Therefore, in this study, the singular value decomposition method is used as a method to obtain the pseudo-inverse matrix. Singular value decomposition of B gives Equation (7) and (8).

$$B = U \cdot S \cdot V^T \tag{7}$$

$$S = \begin{array}{c} \\ \\ \end{array} \begin{array}{c} \begin{array}{cc} h & n-h \end{array} \\ \begin{bmatrix} G_{11} & 0 \\ 0 & 0 \end{bmatrix} \end{array} \qquad G_{11} = \mathrm{diag}(\sigma_1 \quad \sigma_2 \quad \cdots \quad \sigma_h) \tag{8}$$

Note that both U and V are orthogonal matrices, 3m×3m and n×n matrices respectively. Therefore, we obtain the pseudo-inverse of the normalized matrix B using equation (7). From this result, the rank of G_{11}, that is, the rank of B, can be obtained. Since the rank of B is smaller than the number of parameters set in the measuring instrument, the number of parameters can be reduced to the rank by selectively removing redundant parameters. To reduce the number of parameters, we focus on Equation (8). First, since h is the rank of B, the orthogonal matrices U and V are decomposed into two by the rank h, and let $U = [U_1 \quad U_2]$ and $V = [V_1 \quad V_2]$. V_2 corresponds to the singular value 0, and among the elements of each column of V_2, the parameters whose absolute value is close to 1.0 are candidates for deletion. Also, elements in this column that have the same absolute value but different signs mean that the parameters corresponding to those elements overlap each other.

Parameters that overlap with encoder offset values and link lengths, which are the main parameters, are preferentially deleted. However, if it is convenient for calculation and control to delete the main parameters, this is not the case. Also, if two duplicate parameters are rotation angle or displacement, remove one of them. Here, among the postures of the measuring instrument in the absolute coordinate system, one axis of the coordinate system and the rotation axis of the first link, that is, the offset value of the encoder, always overlap.

Published By:
Blue Eyes Intelligence Engineering
and Sciences Publication (BEIESP)

In addition, one of the translational parameters, which is the error between the hand P of the measuring instrument and the reference point Pa, is always a duplicate parameter, so it must be excluded. Therefore, even if it is deleted from the kinematic model first, there is no problem.

This is the procedure for deleting unnecessary redundant parameters, and the kinematic model is reconstructed using this method. Furthermore, the true values of the calibration parameters are obtained using the estimation algorithm based on Newton's method, which will be described below.

C. Parameter Estimation by Newton's Method

As in Section *B*, equation (5) is constructed by substituting the actual measurement value of the reference point P_a at different positions and postures of the measuring instrument, the offset value of the encoder, and the initial value of each parameter.

Next, the pseudo-inverse matrix of *B* is obtained using equation (7) without performing normalization unlike Section *A*.

Here, we replace equation (7) with equation (8) using U_1 and V_1.

$$B = U_1 \cdot G_{11} \cdot V_1^T \tag{8}$$

Furthermore, by transforming equation (8), the pseudo-inverse matrix B^+ is expressed by equation (9).

$$\begin{aligned} B^+ &= V_1 \cdot G_{11}^{-1} \cdot U_1^T \\ G_{11} &= \mathrm{diag}(1/\sigma_1 \quad 1/\sigma_2 \quad \cdots \quad 1/\sigma_h) \end{aligned} \tag{9}$$

Therefore, since equation (5) becomes equation (10), the relation of equation (11) holds between $\boldsymbol{q}_i$ before correction and $\boldsymbol{q}_{i+1}$ after correction.

$$\Delta \boldsymbol{q} = B^+ \cdot \Delta \boldsymbol{r} \tag{10}$$

$$\boldsymbol{q}_{i+1} = \boldsymbol{q}_i + \Delta \boldsymbol{q} \tag{11}$$

By substituting this corrected $\boldsymbol{q}_{i+1}$ into equation (5) and repeating the calculation until $\Delta \boldsymbol{q}$ approaches 0 and converges, the true values of the *n* calibration parameters $\boldsymbol{q}$ are estimated.

However, in practice, this method does not converge. Ishikawa et al. published this method in 1989. The performance of computers at that time was considerably lower than that of today, so the accuracy of calculations was low and the number of significant digits was small. Therefore, it is thought that the latter part of the element of G_{11} became 0 at that time. In the current calculation results, the latter half approaches 0 as much as possible, but does not completely reach 0, so the latter half of the elements of G_{11}^{-1}, which is reciprocal has quite large values. Therefore, the estimation results are not stable and continue to oscillate. Therefore, we solve this problem by using a low-rank approximation that sets the latter half of the elements of G_{11}^{-1} to 0.

IV. ACCURACY VERIFICATION

The contact type three-dimensional measuring instrument sets six-coordinate systems according to the directions of the orthogonal rotation axes of each joint shown in Fig. 3.

Let the position $[x_{p0} \quad y_{p0} \quad z_{p0}]$ from the origin P_0 of the absolute coordinate system be the coordinate system P_1 of J_1. In other words, these three elements are parameters. Next, among the torsion angles at P_1, the y-axis becomes the rotation axis. Therefore, as described in A of Ⅲ, the parameter can be replaced by the offset value of the encoder, so the parameter is set to $[\alpha_1 \quad O_1 \quad \gamma_1]$. Similarly, set the coordinate systems P_2 to P_6 of J_2 to J_6, and set the respective parameters to $[x_{p1} \quad y_{p1} \quad z_{p1}]$, $[O_2 \quad \beta_2 \quad \gamma_2]$, $[x_{p2} \quad y_{p2} \quad z_{p2}]$, $[\alpha_3 \quad \beta_3 \quad \gamma_3]$, $[x_{p3} \quad y_{p3} \quad l_3 + O_3]$, $[O_4 \quad \beta_4 \quad \gamma_4]$, $[x_{p4} \quad y_{p4} \quad z_{p4}]$, $[\alpha_5 \quad O_5 \quad \gamma_5]$, $[x_{p5} \quad y_{p5} \quad z_{p5}]$, $[\alpha_6 \quad \beta_6 \quad O_6]$, $[0 \quad 0 \quad l_6]$, there are 38 initial parameters in total. Also, l_3 is defined because it has a physical length as a link, but it is deleted because it overlaps with O_3 in the end. Table 1 shows the proportionality constants of C_1 to C_6 along with the initial values of these parameters.

Table 1 Initial Parameters and Constant of Proportionality

x_{p0} [m]	y_{p0} [m]	z_{p0} [m]	α_1 [rad]	O_1 [ ]	γ_1 [rad]
0	0	0	0	-3682	0

x_{p1} [m]	y_{p1} [m]	z_{p1} [m]	O_2 [ ]	β_2 [rad]	γ_2 [rad]
0	0	0	676	0	0

x_{p2} [m]	y_{p2} [m]	z_{p2} [m]	α_3 [rad]	β_3 [rad]	γ_3 [rad]
0	0	0	0	0	0

x_{p3} [m]	y_{p3} [m]	l_3 [m]	O_3 [ ]	O_4 [ ]	β_4 [rad]
0	0	0.145	-25165	617	0

γ_4 [rad]	x_{p4} [m]	y_{p4} [m]	z_{p4} [m]	α_5 [rad]	O_5 [ ]
0	0	0	0	0	281

γ_5 [rad]	x_{p5} [m]	y_{p5} [m]	z_{p5} [m]	α_6 [rad]	β_6 [rad]
0	0	0	0	0	0

O_6 [ ]	l_6 [m]
-1886	0.0425

C_1 [ ]	C_2 [ ]	C_3 [ ]	C_4 [ ]	C_5 [ ]	C_6 [ ]
1273.24	1273.24	100000.00	-1273.24	1273.24	1273.24

Next, in order to set the calibration parameters, the reference point P_a $[x_{pa} \quad y_{pa} \quad z_{pa} \quad \alpha_{pa} \quad \beta_{pa} \quad \gamma_{pa}]$ is measured at x_{pa} = -20.0, 0.0, 20.0 mm, y_{pa} = -20.0, 0.0, 20.0 mm, z_{pa} = -373.0, -363.0, -353.0 mm, $\alpha_{pa} = \beta_{pa} = \gamma_{pa} = 0.0$ deg, 27 points. Table 2 shows the measurement results. The resolution of the encoder is 0.045 deg at quadruple multiplication for UN-2000, which detects the rotational direction, and 0.01 mm at quadruple multiplication for DX-025, which detects the translation direction. All measurements were performed at quadruple multiplication.

Published By:
Blue Eyes Intelligence Engineering
and Sciences Publication (BEIESP)

Table 2 Measurement Data for Setting Calibration Parameters

reference point						measured value					
x_{pa} [m]	y_{pa} [m]	z_{pa} [m]	α_{pa} [deg]	β_{pa} [deg]	γ_{pa} [deg]	x_{pa} [m]	y_{pa} [m]	z_{pa} [m]	α_{pa} [deg]	β_{pa} [deg]	γ_{pa} [deg]
-0.020	-0.020	-0.373	0.000	0.000	0.000	-0.02011	-0.01884	-0.37299	0.23	0.13	0.35
-0.020	-0.020	-0.363	0.000	0.000	0.000	-0.02027	-0.01874	-0.36303	0.27	0.13	0.21
-0.020	-0.020	-0.353	0.000	0.000	0.000	-0.02010	-0.01861	-0.35308	0.31	0.09	0.30
0.000	-0.020	-0.373	0.000	0.000	0.000	-0.03900	-0.01945	-0.37294	0.05	0.18	0.18
0.000	-0.020	-0.363	0.000	0.000	0.000	-0.03900	-0.01937	-0.36300	0.05	0.18	0.36
0.000	-0.020	-0.353	0.000	0.000	0.000	-0.03800	-0.01895	-0.35306	0.14	0.18	0.41
0.020	-0.020	-0.373	0.000	0.000	0.000	0.01955	-0.01962	-0.37295	359.87	0.27	0.31
0.020	-0.020	-0.363	0.000	0.000	0.000	0.01971	-0.01951	-0.36303	359.91	0.27	0.49
0.020	-0.020	-0.353	0.000	0.000	0.000	0.01958	-0.01912	-0.35301	359.96	0.27	0.31
-0.020	0.000	-0.373	0.000	0.000	0.000	-0.02030	0.00088	-0.37295	0.13	0.05	359.18
-0.020	0.000	-0.363	0.000	0.000	0.000	-0.02020	0.00086	-0.36303	0.13	0.05	359.14
-0.020	0.000	-0.353	0.000	0.000	0.000	-0.20330	0.00087	-0.35298	0.18	0.09	359.13
0.000	0.000	-0.373	0.000	0.000	0.000	-0.00036	0.00055	-0.37291	0.04	0.14	359.73
0.000	0.000	-0.363	0.000	0.000	0.000	-0.00035	0.00025	-0.36298	360.00	0.13	359.91
0.000	0.000	-0.353	0.000	0.000	0.000	-0.00038	0.00028	-0.35297	0.05	0.13	0.00
0.020	0.000	-0.373	0.000	0.000	0.000	0.01965	0.00045	-0.37292	359.91	0.14	0.76
0.020	0.000	-0.363	0.000	0.000	0.000	0.01974	0.00015	-0.36296	359.87	0.23	0.76
0.020	0.000	-0.353	0.000	0.000	0.000	0.01934	-0.00010	-0.35303	359.87	0.27	0.76
-0.020	0.020	-0.373	0.000	0.000	0.000	-0.02001	0.02034	-0.37301	0.04	0.00	359.14
-0.020	0.020	-0.363	0.000	0.000	0.000	-0.02017	0.02078	-0.36306	0.09	0.00	359.18
-0.020	0.020	-0.353	0.000	0.000	0.000	-0.02030	0.02038	-0.35303	0.09	0.00	359.32
0.000	0.020	-0.373	0.000	0.000	0.000	-0.00033	0.02024	-0.37300	359.95	0.09	359.46
0.000	0.020	-0.363	0.000	0.000	0.000	-0.00032	0.02013	-0.36303	359.95	0.09	359.68
0.000	0.020	-0.353	0.000	0.000	0.000	-0.00031	0.01999	-0.35301	359.95	0.09	359.77
0.020	0.020	-0.373	0.000	0.000	0.000	0.01962	0.02018	-0.37301	359.82	0.18	0.26
0.020	0.020	-0.363	0.000	0.000	0.000	0.01953	0.02011	-0.36305	359.87	0.18	0.26
0.020	0.020	-0.353	0.000	0.000	0.000	0.01965	0.01969	-0.35304	359.82	0.18	359.72

Based on the data in Table 2, unnecessary redundant parameters were deleted using method B in III. The rank of B became 22, and focusing on each column of V_2, redundant parameters were deleted from the B condition of III for the element. However, the rank of B after deletion was 21, and one necessary calibration parameter was missing. This is because the measurement data used to set the calibration parameters contained errors. Therefore, we simply performed a dichotomous method using the rank of B as the evaluation criterion for the parameters that seemed to be questionable. By doing this, we identified the calibration parameters that were deleted mistakenly and narrowed them down to 22.

Finally, the calibration parameters were estimated by Newton's method shown in C of III. Table 3 shows the initial values and estimated results of 22 calibration parameters based on the state of convergence. Among the 38 initial parameters deleted from Table 1, O_2, l_3, and O_6 had initial values, so they were replaced with the initial values of the duplicated calibration parameters α_3, O_3, and γ_5, respectively. This hastened the convergence of Newton's method and reduced the number of estimations.

Table 3 Calibration Parameters

	q_0	q_1	q_2	q_3	q_4	q_5
x_{p0} [m]	0.00000	0.00023	0.00031	0.00031	0.00031	0.00031
y_{p0} [m]	0.00000	-0.00053	-0.00065	-0.00065	-0.00065	-0.00065
z_{p0} [m]	0.00000	-0.04124	-0.04130	-0.04130	-0.04130	-0.04130
O_1 [ ]	-3682.00000	-3682.00000	-3682.00000	-3682.00000	-3682.00000	-3682.00000
γ_1 [rad]	0.00000	-0.00754	-0.00760	-0.00760	-0.00760	-0.00760
z_{p1} [m]	0.00000	-0.00322	-0.00311	-0.00311	-0.00311	-0.00311
γ_2 [rad]	0.00000	-0.00633	-0.00641	-0.00641	-0.00641	-0.00641
α_3 [rad]	-0.53093	-0.52796	-0.52769	-0.52767	-0.52767	-0.52767
β_3 [rad]	0.00000	0.00271	0.00291	0.00289	0.00289	0.00289
y_{p3} [m]	0.00000	0.00109	0.00119	0.00120	0.00120	0.00120
O_3 [ ]	-39665.00000	-39665.00000	-39665.00000	-39665.00000	-39665.00000	-39665.00000
O_4 [ ]	617.00000	617.00000	617.00000	617.00000	617.00000	617.00000
β_4 [rad]	0.00000	-0.00003	-0.00003	-0.00003	-0.00003	-0.00003
γ_4 [rad]	0.00000	-0.00139	-0.00139	-0.00139	-0.00139	-0.00139
x_{p4} [m]	0.00000	-0.00084	-0.00073	-0.00072	-0.00072	-0.00072
z_{p4} [m]	0.00000	-0.00159	-0.00146	-0.00146	-0.00146	-0.00146
α_5 [rad]	0.00000	-0.00003	-0.00003	-0.00003	-0.00003	-0.00003
O_5 [ ]	281.00000	281.00000	281.00000	281.00000	281.00000	281.00000
γ_5 [rad]	1.48126	1.47920	1.47920	1.47920	1.47920	1.47920
α_6 [rad]	0.00000	-0.00016	-0.00016	-0.00016	-0.00016	-0.00016
β_6 [rad]	0.00000	0.00016	0.00016	0.00016	0.00016	0.00016
l_6 [m]	0.04250	0.00608	0.00578	0.00578	0.00578	0.00578

Here, we verified the accuracy improvement using the obtained calibration parameters. In the verification, a measurement point P different from the reference point P_a used in setting the calibration parameters was used. The eight-measurement points $P\begin{bmatrix} x_p & y_p & z_p & \alpha_p & \beta_p & \gamma_p \end{bmatrix}$ are a combination of x_p = -20.0, 20.0 mm, y_p = -15.0, 15.0 mm, z_p = -373.0, -353.0 mm, $\alpha_p = \beta_p = \gamma_p = 0.0$ deg. Also, measurements were made with and without calibration. Table 4 shows the measurement results. The accuracy error range required for this instrument is ±1.0 mm for position and ±1.0 deg for angle. In the results of Table 4, the accuracy of the positions x_p, y_p, and z_p after calibration are generally within the range of ±1.0 mm. In particular, the variation corresponding to the standard deviation is smaller than before the calibration, and the effect of the calibration appears remarkably. On the other hand, the angle error between α_p and β_p is significantly worse, around ±3.0 deg. This is because the calibration method used in the study is targeted only to the position and does not have any restrictions on the angle. Regarding this problem, it is necessary to provide a new calibration method for angles. However, for the target position component, it was shown that the method of applying the calibration method of the manipulator presented this time to the measuring instrument is effective.

Table 4 Verification Results of the Calibration

without calibration

reference point						measured value						error					
x_{pa} [m]	y_{pa} [m]	z_{pa} [m]	α_{pa} [deg]	β_{pa} [deg]	γ_{pa} [deg]	x_{pa} [m]	y_{pa} [m]	z_{pa} [m]	α_{pa} [deg]	β_{pa} [deg]	γ_{pa} [deg]	x [m]	y [m]	z [m]	α [deg]	β [deg]	γ [deg]
-0.020	-0.015	-0.373	0.000	0.000	0.000	-0.02034	-0.01454	-0.37303	-0.04371	0.09059	-0.76769	-0.00034	0.00046	-0.00003	-0.04371	0.09059	-0.76769
-0.020	-0.015	-0.353	0.000	0.000	0.000	-0.02037	-0.01437	-0.35306	-0.08843	0.13591	-0.59065	-0.00037	0.00063	-0.00006	-0.08843	0.13591	-0.59065
0.020	-0.015	-0.373	0.000	0.000	0.000	0.01870	-0.01529	-0.37303	0.27322	0.35719	-0.60217	-0.00130	-0.00029	-0.00003	0.27322	0.35719	-0.60217
0.020	-0.015	-0.353	0.000	0.000	0.000	0.01848	-0.01502	-0.35314	0.13829	0.44892	-0.45923	-0.00152	-0.00002	-0.00014	0.13829	0.44892	-0.45923
0.020	0.015	-0.373	0.000	0.000	0.000	0.01959	0.01412	-0.37309	0.27145	0.22262	-0.51216	-0.00041	-0.00088	-0.00009	0.27145	0.22262	-0.51216
0.020	0.015	-0.353	0.000	0.000	0.000	0.01876	0.01374	-0.35319	0.27267	0.40283	-0.46844	-0.00124	-0.00126	-0.00019	0.27267	0.40283	-0.46844
-0.020	0.015	-0.373	0.000	0.000	0.000	-0.02005	0.01506	-0.37308	0.04523	0.04468	-0.40232	-0.00005	0.00006	-0.00008	0.04523	0.04468	-0.40232
-0.020	0.015	-0.353	0.000	0.000	0.000	-0.02028	0.01465	-0.35318	0.04490	-0.00028	-0.35707	-0.00028	-0.00035	-0.00018	0.04490	-0.00028	-0.35707
								average of error				-0.00069	-0.00021	-0.00010	0.11420	0.21281	-0.51997
								standard deviation of error				0.00053	0.00060	0.00006	0.13751	0.16098	0.12242

with calibration

reference point						measured value						error					
x_{pa} [m]	y_{pa} [m]	z_{pa} [m]	α_{pa} [deg]	β_{pa} [deg]	γ_{pa} [deg]	x_{pa} [m]	y_{pa} [m]	z_{pa} [m]	α_{pa} [deg]	β_{pa} [deg]	γ_{pa} [deg]	x [m]	y [m]	z [m]	α [deg]	β [deg]	γ [deg]
-0.020	-0.015	-0.373	0.000	0.000	0.000	-0.02014	-0.01530	-0.37303	3.55312	3.30560	-0.71556	-0.00014	-0.00030	-0.00003	3.55312	3.30560	-0.71556
-0.020	-0.015	-0.353	0.000	0.000	0.000	-0.02010	-0.01511	-0.35307	3.67722	3.52421	-0.53512	-0.00010	-0.00011	-0.00007	3.67722	3.52421	-0.53512
0.020	-0.015	-0.373	0.000	0.000	0.000	0.01918	-0.01543	-0.37304	-3.18416	-2.77766	-0.53727	-0.00082	-0.00043	-0.00004	-3.18416	-2.77766	-0.53727
0.020	-0.015	-0.353	0.000	0.000	0.000	0.01907	-0.01516	-0.35315	-3.58109	-2.93819	-0.40018	-0.00093	-0.00016	-0.00015	-3.58109	-2.93819	-0.40018
0.020	0.015	-0.373	0.000	0.000	0.000	0.02000	0.01397	-0.37309	-3.17907	-2.91726	-0.43476	0.00000	-0.00103	-0.00009	-3.17907	-2.91726	-0.43476
0.020	0.015	-0.353	0.000	0.000	0.000	0.01935	0.01369	-0.35319	-3.44533	-2.98354	-0.38800	-0.00065	-0.00131	-0.00019	-3.44533	-2.98354	-0.38800
-0.020	0.015	-0.373	0.000	0.000	0.000	-0.01985	0.01436	-0.37306	3.62160	3.28283	-0.34249	0.00015	-0.00064	-0.00006	3.62160	3.28283	-0.34249
-0.020	0.015	-0.353	0.000	0.000	0.000	-0.02007	0.01398	-0.35316	3.93180	3.52560	-0.29529	-0.00007	-0.00102	-0.00016	3.93180	3.52560	-0.29529
								average of error				-0.00032	-0.00063	-0.00010	0.17426	0.25270	-0.45608
								standard deviation of error				0.00039	0.00042	0.00006	3.52524	3.15839	0.12607

Published By:
Blue Eyes Intelligence Engineering and Sciences Publication (BEIESP)

V. CONCLUSION

In this paper, to solve the error problem of the contact type three-dimensional position measuring instrument, a method of applying the calibration method used for the manipulator to the measuring instrument was presented. Also, the kinematic model and its calibration parameters were explained, and a method of deleting unnecessary parameters with redundancy and parameter estimation by Newton's method was presented. Furthermore, in a comparative verification using a measuring instrument, we confirmed that the positional accuracy after calibration was within a range of approximately ±1.0 mm, and that the variation was also within a range of ±0.5 mm. It was shown that the proposed method is effective. To aim for even higher accuracy in the future, we present the following two issues.

1. Calibration for Angles

In this paper, the method focuses only on the position component, and by extending it to the angle component, it will be possible to perform a more accurate measurement in three-dimension space. Parameter estimation by Newton's method can also be applied to the angle component, so deriving the Jacobian matrix for the angle component is a major issue.

2. Calibration of the Test Field

The calibration presented this time also includes external parameters, which are errors caused by the relationship between the installation positions of the measuring instrument and the 6-axis stage. Therefore, when verifying the pipe inspection robot, the 6-axis stage replaces the test field, so the external parameters of the error also change. In other words, it is necessary to establish a method to re-estimate only the extrinsic parameters of the errors while leaving the intrinsic parameters of the errors of the measuring instrument itself unchanged.

REFERENCES

1. Japan institute of wastewater engineering technology, “Development foundation survey of sewerage facilities management robot”, Sewer new technology Annual report of the Institute, 1992, pp.43-52.
2. Rome, E., Hertzberg, J., Kirchner, F., Licht, U. and Christaller, T., “Towards Autonomous Sewer Robots: the MAKRO Project”, Urban Water, Vol. 1, 1999, pp. 57-70. [CrossRef]
3. Streich, H. and Adria, O., “Software approach for the autonomous inspection robot MAKRO”, in Proceedings of the 2004 IEEE International Conference Robotics and Automation, 2004, pp. 3411-3416. [CrossRef]
4. Birkenhofer, C., Regenstein, K., Zöllner, J. M. and Dillmann, R., “Architecture of multi-segmented inspection Robot KAIRO-II”, DOI: 10.1007/978-1-84628-974-3_35, In book: Robot Motion and Control, 2007, pp.381-389. [CrossRef]
5. Ayaka, N., Kazutomo, F., Toshikazu, S., Mikio, G. and Hirofumi M., “Prototype design for a piping inspection robot”, 43rd Graduation Research Presentation Lecture of Student Members of the JSME, 2013, 716.
6. Kazutomo, F., Yoshiki, I. and Hirofumi M., “Modularization for a piping inspection robot”, 2013 Symposium on System Integration, 2013, pp.1297-1300.
7. Kazutomo, F., Toshikazu, S., Mikio, G., Yoshiki, I. and Hirofumi M., “Miniaturization of the piping inspection robot by modularization”, 44th Graduation Research Presentation Lecture of Student Members of the JSME, 2014, 613.
8. Hirofumi, M., Takuya, K., Kazutomo, F., Yoshiki, I., Toshikazu, S. and Mikio, G., “Research and development about a piping inspection robot - Report1: Prototype design for a miniaturization -”, Bulletin of National Institute of Technology, Yuge College, Vol. 36, 2014, pp.79-82.
9. Hirofumi, M., Yoshiki, I., Toshikazu, S. and Mikio, G., “Research and development about a piping inspection robot - Report2: Prototype design for maintenance improvement -”, Bulletin of National Institute of Technology, Yuge College, Vol. 37, 2015, pp.75-79.
10. Hirofumi M., Ryota, K., “Development of a small autonomous pipe inspection robot (Modularization of hardware using the technique of wooden mosaic work)”, Transactions of the Japan Society of Mechanical Engineers, Vol.82, No.839, 2016, pp.1-16. [CrossRef]
11. Hirofumi M., “Automatic Compensation of the Positional Error Utilizing Localization Method in Pipe”, International Journal of Recent Technology and Engineering (IJRTE), Vol.9, No.6, 2021, pp.151-157. [CrossRef]
12. Yuki, Y., Yoshiki, I., Hirofumi, M., “Self-localization Measurement of the Piping Inspection Robot by a ARtoolkit”, Transactions of the Japan Society of Mechanical Engineers, No. 165-1, 2016, 502.
13. Ayano, T., Hirofumi, M., “Accuracy Improvement of the Measuring Instrument for the Piping Inspection Robot”, The Japan Society of Mechanical Engineers Chugoku-Shikoku Branch, the 47th Conference on the Graduation Thesis for Undergraduate Students,2017, 921.
14. Ayano, T., Hirofumi, M., “Tilt Adjustment to Measuring Instrument for Piping Inspection Robot”, Transactions of the Japan Society of Mechanical Engineers, No. 185-1, 2018, 1304. [CrossRef]
15. Keita I., Hirofumi M., “Hardware Design for the Contact Type Measuring Instrument”, The Japan Society of Mechanical Engineers Chugoku-Shikoku Branch, the 52nd Conference on the Graduation Thesis for Undergraduate Students, 2022, 11b4.
16. Ibuki T., Hirofumi M., “Data Reception of the Contact Type Measuring Instrument using BLE”, Transactions of the Japan Society of Mechanical Engineers, No. 225-1, 2022, 09a1.
17. Kohei S., Hirofumi M., “Posture Measurement of a Robot using the Contact Type Measuring Instrument”, Transactions of the Japan Society of Mechanical Engineers, No. 225-1, 2022, 09a2.
18. Hirofumi M., “A Contact Type Three Dimensional Position Measuring Instrument for Verification of a Piping Inspection Robot”, International Journal of Recent Technology and Engineering (IJRTE), Vol.10, No.6, 2022, pp.65-72.
19. Masaru I., Shigeyuki S., Masayoshi K., Yoshio M., “Robot Manipulator Calibration for 3D Model Based Robot Systems”, Journal of the Robotics Society of Japan, Vol.7, No.2, 1989, pp.74-83. [CrossRef]

AUTHOR PROFILE

Hirofumi Maeda is Associate Professor in the Information Science and Technology Department at National Institute of Technology (KOSEN), Yuge College. Dr. Maeda’s research focuses on the practical application of mechanical engineering, namely, developing rescue robots, pipe inspection robots and natural language processing. Dr. Maeda previously served as a researcher at the NPO International Rescue System Institute. Dr. Maeda is currently a member of the Japan Society of Mechanical Engineers, the Robotics Society of Japan, the Japan Association for College of Technology, and the Japan Institute of Marine Engineering. Dr. Maeda has published 11 peer-reviewed papers and presented 81 papers. In addition, Dr. Maeda received two awards at academic conferences and 14 external funds.

Retrieval Number: 100.1/ijrte.E73840111523
DOI: 10.35940/ijrte.E7384.0111523
Journal Website: www.ijrte.org

Published By:
Blue Eyes Intelligence Engineering and Sciences Publication (BEIESP)